JOURNAL OF AGRICULTURAL AND FOOD CHEMISTRY

Article

pubs.acs.org/JAFC

# Structural Elucidation of Lignin Polymers of *Eucalyptus* Chips during Organosolv Pretreatment and Extended Delignification

Jia-Long Wen,[†] Shao-Long Sun,[†] Tong-Qi Yuan,[†] Feng Xu,[†] and Run-Cang Sun[†,‡,*]

[†]Beijing Key Laboratory of Lignocellulosic Chemistry, Beijing Forestry University, Beijing, China

[‡]State Key Laboratory of Pulp and Paper Engineering, South China University of Technology, Guangzhou, China

Supporting Information

**ABSTRACT:** Effective delignification of lignocelluloses is a very important to guarantee the economic feasibility of organosolv-based biorefinery. *Eucalyptus* chips were successively subjected to organosolv pretreatment (AEOP) and extended delignification (ED) process in the present study. The effects of delignification processes were scientifically evaluated by component analysis, SEM, and CP-MAS NMR techniques. It was found that the integrated process of organosolv pretreatment and subsequent delignification resulted in an effective delignification. The fundamental chemistry of the lignin obtained after these processes was thoroughly investigated by FT-IR, multidimensional NMR ($^{31}$P-, $^{13}$C-, and 2D-HSQC NMR), and GPC techniques. It was observed that an extensive cleavage of aryl ether linkages, ethoxylation, and some condensation reactions occurred in AEOP process, while $\alpha$-oxidation mainly took place in alkaline hydrogen peroxide (AHP) process. It is believed that better understanding the fundamental chemistry of lignin facilitates the optimization of the delignification process. More importantly, well-defined of lignin polymers will facilitate their value-added applications in current and future biorefineries.

**KEYWORDS:** *delignification, lignin, NMR, β-O-4 linkages, structural elucidation*

## INTRODUCTION

Lignocellulosic biomass (LCB) can provide sustainable feedstock, which are mainly composed of cellulose, hemicelluloses, and lignin. The renewable carbon source can be used for the production of biofuels, energy, and value-added products and chemicals.[1,2] However, most biorefineries plant currently focus on the utilization of cellulose and hemicelluloses, whereas the lignin produced or remained is deemed as a waste residue due to its lower purity and chemical reactivity. To increase the overall economic feasibility of a biorefinery mode, it is very important to obtain high purity lignin with commendable chemical reactivity. In addition, the exploitation of a lignin-based coproduct also depends on the inherent structures and chemical reactivity of the lignin polymers.

Lignin is a thermoplastic three-dimensional and amorphous polymer, comprising of different linkages, such as *β-O*-4, *α-O*-4, *β*−*β*, *β*-5, *β*-1, 5−5, 4-*O*-5, and dibenzodioxocin linkages, depending on the LCB species.[3] The inherent complexity of lignin and its structural transformations make it difficult to develop an efficient method to effectively isolate lignin polymers as starting feedstock for subsequent utilizations. Thus, a comprehension of structural transformations during a biorefinery process is of vital importance.[4] So far, the structural analysis of lignin polymer is based on wet chemical methods (thioacidolysis, nitrobenzene oxidation, and derivatization followed by reductive cleavage).[5] However, these methods cannot panoramically observe the whole lignin molecular because noncondensed lignins are degraded and detected by these methods. Thanks to the advances nuclear magnetic resonance (NMR), the knowledge of lignin has been substantially enlarged and extended.[6−8]

Up to now, several lignin preparations based on extraction and isolation procedures are available. The lignin polymers (kraft lignin, alkali lignin, and ligninsulfonates lignin) have different chemical functionalizations, physical properties, and address a range of molecular masses, and thus they can be used for developing general products and chemicals.[9] However, the complex structures and wide range of molecular masses undoubtedly limited their further value-added utilizations. Apart from these lignin sources, autocatalyzed organosolv lignin (AEOL) have a high purity, higher chemical reactivity, small molecular weights.[10] In our previous study, the isolated AEOL from southwest birch wood has been investigated as compared to cellulolytic enzyme lignins (CELs) isolated from control and pretreated biomass.[11] Similarly, the kinetic study of autocatalyzed ethanol pulping of *Eucalyptus globules* was conducted to evaluate the delignification effect.[12] Recently, researchers have showed that residual lignin content in the organosolv pretreated *Eucalyptus* wood varies from 6.8 to 13.8% at different pretreated conditions in bioethanol production.[13] It is well-known that the structural analysis of the residual lignin polymers are important in extended delignification.[14,15] However, no investigations were made to elucidate the structural transformations of lignin polymers during autocatalyzed ethanol organosolv pretreatment (AEOP) and extended delignification (ED).

Extended delignification is needed to further fractionate or remove the residual lignin in AEOP crude pulp. A previous study reported that alkaline ethanol treatment (AE) is a suitable method to extract lignin polymers from LCB or pretreated LCB.[16] Alternatively, alkaline hydrogen peroxide (AHP)

Received: August 21, 2013
Revised: October 27, 2013
Accepted: October 29, 2013
Published: October 29, 2013





dx.doi.org/10.1021/jf403717q | J. Agric. Food Chem. 2013, 61, 11067−11075

pretreatment has been considered as a good chemical pretreatment to remove lignin from biomass.[17,18] Moreover, AHP has been successfully applied to isolate hemicelluloses and lignin from herbaceous biomass at mild conditions.[19] Based on the above enlightenments, two parallel delignification processes (AE and AHP) were applied to the AEOP pretreated *Eucalyptus* wood (crude-pulp) to isolate lignin polymers and obtain purified pulps.

To understand the delignification mechanism during AEOP and subsequent extended delignification, and provide fundamental chemistry for optimizing the whole process, *Eucalyptus* chips was first pretreated with 50% aqueous ethanol at 200 °C for 1 h, obtaining autocatalyzed organosolv lignin (AEOL) and crude pulp. Two extended delignification processes were applied to the crude pulp to obtain the lignin polymers and purified pulp, and the "lignin" was also isolated from *Eucalyptus* wood and crude pulp, respectively. The integrated delignification process has been investigated by component analysis, SEM, and CP-MAS NMR techniques. Moreover, the relationship between lignin structures and the reactivity was investigated by gel permeation chromatography (GPC), Fourier transform infrared (FT-IR), quantitative $^{13}C$ NMR, two-dimensional heteronuclear single quantum coherence (2D-HSQC) NMR, and $^{31}P$ NMR spectroscopies. The fundamental chemistry of the lignin will provide valuable insights into the integrated delignification and future biorefinery.

## MATERIALS AND METHODS

**Materials.** *Eucalyptus* chips (2 × 0.5 × 0.5 cm) was prepared from *Eucalyptus grandis* × *Eucalyptus urophylla* wood (5 years old, harvested from Guangxi province, China). The composition of *Eucalyptus* wood was 37.5% glucan, 16.2% xylan, 0.26% arabinan, 0.99% galactan, 32.3% Klason lignin, 2.0% acid-soluble lignin, which was analyzed by the standard of NREL.[20]

**Integrated Delignification Process.** The scheme of integrated delignification is depicted in Figure 1. The integrated process was

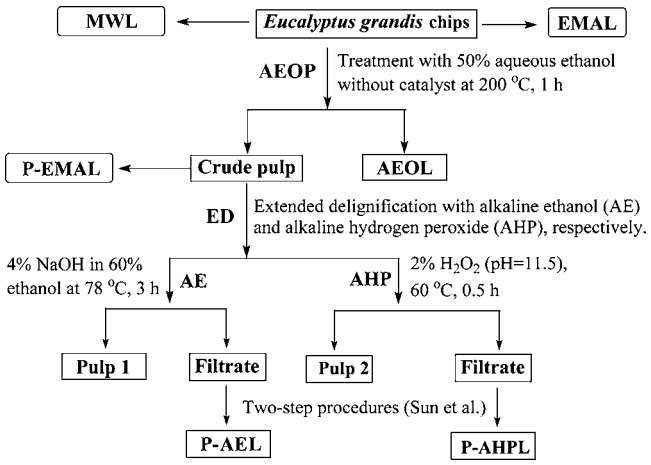


**Figure 1.** Scheme of the integrated delignification process.

composed of AEOP and ED. First, *Eucalyptus* chips (50 g) were treated with 50% aqueous ethanol at 200 °C for 1 h (1:10, solid/liquid). The pretreated *Eucalyptus* chips were filtered and washed using the same aqueous ethanol (150 mL) for several times. The mixed filtrates were concentrated to 150 mL at 50 °C under reduced pressure, poured into 5−10 volumes of water to precipitate the dissolved lignin (AEOL). After being filtered, collected, and washed with acidic water (pH 2.0) several times, purified AEOL was obtained by centrifugation and freeze-drying. The ED of crude pulp was both achieved by alkaline ethanol (AE) and alkaline hydrogen peroxide (AHP) pretreatments. Detailedly, 10 g crude pulp was treated with 250 mL of 4% NaOH in 60% ethanol at 78 °C for 3 h. The resulted liquid was used to isolate lignin (P-AEL) according to a recent publication.[16] AHP delignification procedure was accomplished by extracting 10 g crude pulp with 250 mL 2% $H_2O_2$ (pH 11.5, adjusted with NaOH) at 60 °C for 0.5 h. The AHP lignin (P-AHPL) from crude pulp was also isolated according to previous literatures.[17,19]

**Isolation of "Original Lignin" from Control and Pretreated *Eucalyptus* Wood.** To investigate the original lignin structures of the control and pretreated *Eucalyptus* wood, original lignin should be isolated from control *Eucalyptus* Wood, such as milled wood lignin (MWL) and enzymatic mild acidolysis lignin (EMAL). MWL was isolated based on the classic procedure developed by Björkman,[21] while EMAL was isolated based on a publication with some modifications.[15] The extractive-free *Eucalyptus* wood (30 g, 40−60 mesh) was milled (5 h) in a Fritsch planetary ball mill according to a previous publication.[22] Ball-milled wood was divided into two parts. Ten g ball-milled wood was used for MWL isolation and another 10 g ball-milled wood was used to prepare EMAL.[15,22] To further purify the obtained EMAL, the EMAL was dissolved into 90% acetic acid (1:20), after centrifuging, the lignin solution was dripped into volumes of water (5−10 volumes, pH 2.0) under stirring. After standing, centrifuging and freeze-drying, the purified EMAL from ball-milled *Eucalyptus* wood was obtained. The preparation of "EMAL" from crude pulp was similar to that of ball-milled wood as above-described, named as "P-EMAL".

**Physicochemical Characterization of the Substrates after Integrated Delignification.** CP-MAS $^{13}C$ NMR spectra of different substrates were obtained using a Bruker AVIII 400.M spectrometer (Germany) as previously.[22] X-ray diffraction patterns were obtained with an XRD-6000 instrument (Shimadzu, Japan).[22] Changes in morphology before and after different pretreatments were observed by SEM (S-3400N, HITACHI, Japan).[22]

**Characterization of the Lignin Polymers.** The compositions of the substrates were analyzed using the Laboratory Analytical Procedure (LAP) for biomass provided by NREL.[20] The associated carbohydrates in these lignin samples were measured based on a previous literature.[10] FT-IR spectra of lignin preparations were obtained using a Thermo Scientific Nicolet iN10 FT-IR microscope as previously.[23] NMR spectra were conducted on a Bruker AVIII 400 MHz spectrometer.[23] For the quantitative $^{13}C$ NMR experiments (Program: C13IG), 140 mg of lignin was dissolved in 0.5 mL of DMSO-$d_6$, 20 $\mu$L of chromium(III) acetylacetonate (0.01 M) was added, the parameters were used as follows: The pulse angle (30°); acquisition time (1.4 s); $d_1$ (2s); data points (64 K), and NS (30000).[23] For 2D-HSQC spectra, the Bruker pulse program "hsqcetgpsi" was used and the parameters used is listed as below: The number of collected complex points was 1 K for the $^1H$ dimension with $d_1$ (2 s), number of scanning is 64, and 256 time increments were always recorded. Quantitative $^{31}P$ NMR spectra were conducted according to the literatures.[23−25] The standard $^{31}P$ experiment was selected from Bruker Program Library and the parameters used were listed as follows, the 30° pulse angle; 2 s relaxation delay ($d_1$); 64 K data points, and 1024 scans.

## RESULTS AND DISCUSSION

**Morphology Characteristics of Crude Pulp and Bleached Pulp.** Effective delignification is of vital importance in obtaining high-purity lignin and cellulose. During the integrated processes, crude pulp and bleached pulp were obtained after AEOP and extended delignification processes. The morphology characteristics of *Eucalyptus* chips after the pretreatments can be obtained by SEM and the pictures were illustrated in Supporting Information Figure S1. As starting material, *Eucalyptus* wood chips, was not suitable for SEM scanning because of its big size. After AEOP process, crude pulp was obtained. It was observed that partly dissociative

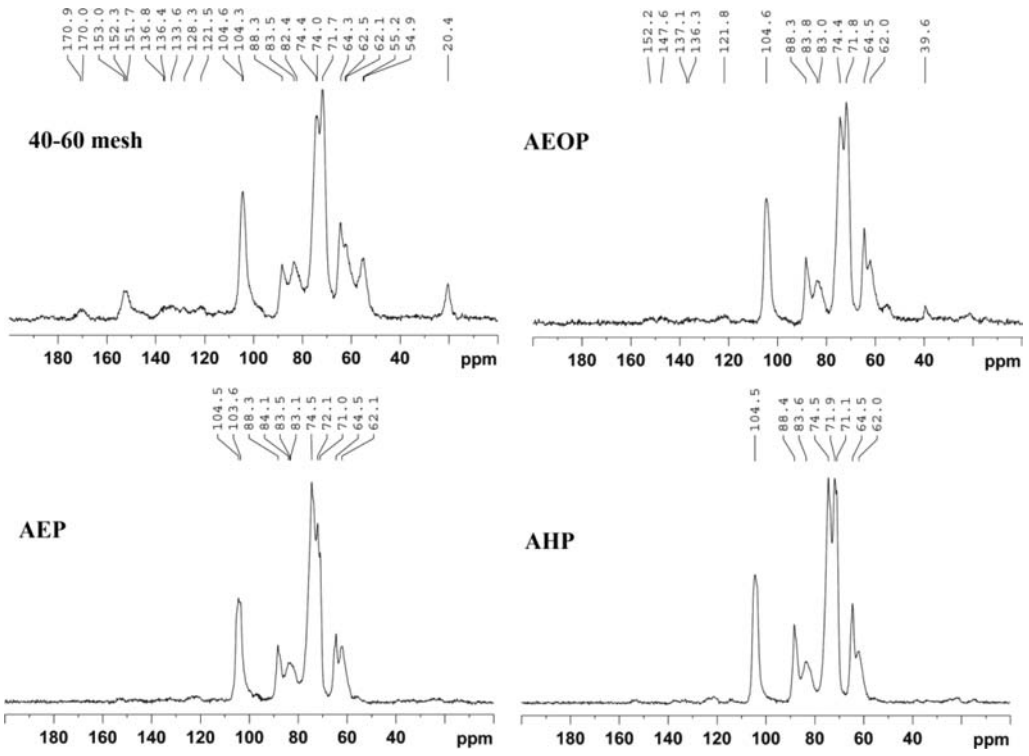


**Figure 2.** CP-MAS $^{13}C$ NMR spectra of pretreated *Eucalyptus* wood chips.

*Eucalyptus* fibers were obtained (Supporting Information Figure S1, upper-left and top-right). In addition, lignin particles were deemed to be deposited on the surface of fibers. It was reported that lignin molecules in wood was cleaved and dissolved in the liquor during organosolv pulping. Some lignin precipitated since that the solubility of lignin in the ethanol liquor was reduced at the lowered temperature.[26] Moreover, a small amount of fiber bundle (Supporting Information Figure S1, upper-right) still existed, suggesting that the delignification of AEOP process was not sufficient and extended delignification was needed. After AE and AHP process, the crude pulp showed typical morphology characteristics of bleached pulp. For example, the fully dissociated fibers implied that the fine pulp was formed. No visible particles were found on the surface of the AE and AHP treated pulp, suggesting that both of the methods greatly removed lignin, as revealed by the subsequent composition analysis of the pretreated *Eucalyptus* chips. Moreover, pits in cell wall were clearly visible. In short, these observed morphological features indicated that the integrated process was an effective delignification method.

**Characterization of Different Substrates after whole Delignification Process.** To investigate the effects of different pretreatments on the crystallinity of the *Eucalyptus* chips, the crystallinity indexes (CrI) of all the samples are shown in Supporting Information Figure S2. As shown, the control wood (40−60 mesh) has a CrI of 40.78%, while the CrI for the crude pulp after AEOP was 51.61%, which was enhanced greatly after the process, suggesting that amorphous hemicelluloses and lignin were significantly removed after the pretreatment. However, after AE (45.74%) and AHP (50.76%) processes, the CrI was slightly decreased as compared to the crude pulp (51.61%), indicating of the swelling action of alkaline treatments. Coincidentally, the aqueous alkaline pretreatment resulted in a reduction in the crystallinity and crystallite size of cellulose.[27]

Solid $^{13}C$ NMR spectra of different substrates were used to track the structural transformations during the pretreatment and delignification process (Figure 2). For example, the 40−60 mesh control wood presented a typical spectral pattern of lignocelluloses. The signals at 172.6 and 20.7 ppm are predominantly attributed to the carbonyl carbons and methyl carbons in acetyl group of hemicelluloses.[22] The noticeable signals (60.0 and 110.0 ppm) represents for the carbons of carbohydrate polymer, mainly cellulose.[22] The signals for lignin polymer were observed at 152.6, 147.6, 133.2, 121.6, 114.2, and 55.0 ppm, which is represented for $S_{3,5}$ (etherified), $S_{3,5}$ (nonetherified), $S_1/S_4$ (nonetherified), $G_6$, $G_5$, and $OCH_3$ in lignin, respectively.[22] After AEOP, it was found that signals for lignin and hemicelluloses were largely reduced (152.6, 55.0, and 20.7 ppm), implying that the most of lignin and hemicelluloses were removed after the AEOP process. In addition, the partially decreased etherified $S_{3,5}$ is indicative of the cleavage of the aryl ether bonds ($\beta$-O-4) of lignin after the pretreatment. Subsequent delignification with AE and AHP processes further removed most of residual lignin in pulp, as revealed by the disappeared signals for lignin in the corresponding spectra.

To further investigate the relative crystallinity index (RCrI) calculated from CP-MAS NMR spectra, amplifying CP-MAS NMR spectra of control wood and different substrates are shown in Supporting Information Figure S3. For the control wood (40−60 mesh), the RCrI was 0.36, while it was climbed to 0.48 after AEOP. However, the RCrI for the AE treated pulp (pulp 1) was decreased to 0.46 due to the alkali treatment, as supported by the XRD results. The RCrI of pulp 2 (Figure 1) was increased to 0.50 after AHP process, suggesting that the AHP process was an effective method to obtain bleached pulp with similar RCrI as compared to commercial microcrystalline cellulose (MCC) (Supporting Information Figure S4). This purified pulp could be used as an ideal starting feedstock for preparing MCC.

**Chemical Composition of the Pretreated Substrates, Yield and Sugar Analysis of the Lignin Polymers.** The effects of pretreatments could be reflected by the evolution of chemical composition in different substrates during the integrated process (Table 1). The sugar analysis revealed that

**Table 1. Chemical Composition of Pretreated *Eucalyptus* Chips during the Integrated Delignification**

| composition | raw material | crude pulp | AE (pulp 1) | AHP (pulp 2) |
|---|---|---|---|---|
| glucan | 37.5 | 65.4 | 78.5 | 82.7 |
| xylan | 16.2 | 6.9 | 5.7 | 8.3 |
| arabinan | 0.3 | ND | ND | ND |
| galactan | 1.0 | ND | ND | ND |
| klason lignin | 32.3 | 11.5 | 5.5 | 0.7 |
| acid-soluble lignin | 2.0 | 3.0 | 2.4 | 1.5 |

glucan and xylan were the dominant constituents in the original *Eucalyptus* wood, while arabinan and galactan were only presented in minor quantities. After the AEOP process, the content of glucan was increased to 65.4% based on crude pulp. The glucan content was further increased to 78.5% and 82.7% in AE-treated and AHP-treated pulp, respectively. By contrast, the content of xylan in pulp was decreased greatly after AEOP and extended delignification as compared to original *Eucalyptus* wood. Take "Klason Lignin, KL" content for example, the KL content in the raw material was 32.3%, while it was greatly reduced to 11.5% in the crude pulp, suggesting that the effectiveness of delignification during AEOP process. Further delignification with AE and AHP processes removed most of lignin in the crude pulp. The KL contents in AE and AHP treated pulp (pulp 1 and pulp 2) were 5.4% and 0.7%, respectively. The fact suggested that AHP process was an effective delignification method.

To observe the structural transformations of lignin during integrated delignification process, the "original lignin" was isolated from different substrates with diverse yields and associated carbohydrates (Supporting Information Table S1, the yield was calculated based on the total lignin in respective substrate). For example, MWL was isolated from *Eucalyptus* wood with a yield of 5%, while EMAL was isolated with a yield of 20%. The AEOP process collected high yield and purity AEOL (56%). The original lignin "P-EMAL" was also extracted with a higher yield of 34%. Subsequent delignification with AE and AHP processes collected 37% and 20% lignin, respectively. The carbohydrate content in the lignin polymers varied from 0.97 to 4.17% (Supporting Information Table S1) and the low associated carbohydrate will facilitate the subsequent structural analysis of lignin.

**Structural Elucidation of Lignin Polymers.** FT-IR Spectra. FT-IR spectra can be used to investigate the structural fragments of the lignin polymers. For comparison, the spectra of MWL, EMAL, and AEOL are plotted in Supporting Information Figure S5. The spectra of all lignin samples showed the C═O stretch, such as 1720 $cm^{-1}$ (unconjugated C═O stretch) and 1660 $cm^{-1}$ (conjugated C═O stretch). Particularly, the conjugated units in lignin were probably related to oxidation at $\alpha$-position of side-chain of lignin during these processes. The similar spectra patterns of aromatic skeletal vibrations in the lignin samples (1603, 1513, and 1421 $cm^{-1}$ and 1460 $cm^{-1}$) suggested that the basic aromatic structures of lignin were not changed during these processes. The band at 1270 $cm^{-1}$ represented guaiacyl units plus C═O stretch, while syringyl and condensed guaiacyl units showed bands at 1326 $cm^{-1}$. In addition, the C−C plus C═O stretch was observed at 1224 $cm^{-1}$. Other bonds at 1030 $cm^{-1}$, 830 $cm^{-1}$, could also be safely assigned according to a previous publication.[28] Besides the similar bonds appeared in the FT-IR spectra of MWL, EMAL, and AEOL, the obvious differences in the spectra of P-EMAL, P-AEL, and P-AHPL (Supporting Information Figure S5) could be found at the regions between 1630 and 1720 $cm^{-1}$. The strong bond at 1717 $cm^{-1}$ in P-EMAL and P-AEL suggested that nonconjugated C═O were abundant in the lignin samples. By contrast, the bond for nonconjugated C═O was reduced greatly while conjugated C═O bond was increased in P-AHPL, implying that $\alpha$-carbonyl group was decreased during AHP process. However, the differences presented in the FT-IR spectra are still needed to be confirmed by following NMR techniques.

Quantitative $^{13}C$ NMR Spectra. To compare the detailed structural differences among these lignin polymers after the integrated process, the $^{13}C$ NMR spectra of lignin samples were conducted (Supporting Information Figures S6 and S7). The original lignin "EMAL" was used as a standard to investigate structural transformations of lignin during the integrated process because EMAL is an ideal sample represented for original lignin due to its higher yield and unaltered structures.[15] The detail assignments of EMAL could be achieved by a recent publication about NMR characterization of lignin.[8] For example, the obvious signals were listed, such as, 152.7−152.3 ppm (etherified $S_{3/5}$, mainly $\beta$-*O*-4), 149.3 ppm (etherified $G_3$), 148.0−147.1 ppm ($G_4$ in $\beta$−$\beta$ units, nonetherified $S_{3,5}$ units, nonether $G_3$ units), 145.5 ppm (nonetherified $G_4$), 138.2 ppm (etherified $S_4$),135.0−134.4 ppm (etherified $S_1$ or $G_1$), 119.2 ppm ($G_6$), 114.9 ppm ($G_5$), 111.5 ppm ($G_2$), and 104.4−103.4 ppm ($S_{2,6}$), respectively.[11] In addition, the $C_\beta$, $C_\alpha$, and $C_\gamma$ of $\beta$-*O*-4 linkages in the lignin fractions could be distinguished by 86.2, 72.4, and 60.2 ppm, respectively. The structural transformation of lignin during AEOP process could be obtained by comparing the corresponding spectra of EMAL and AEOL (Supporting Information Figure S6, I). For instance, the signals of $\beta$-*O*-4 and etherified $S_{3,5}$ units were significantly decreased in AEOL, while the signals of nonetherified $S_{3,5}$ and $G_{3,4}$ lignin were increased in AEOL as compared to EMAL, suggesting that the major aryl ether linkages ($\beta$-*O*-4 linkages) were mostly cleaved after AEOP process. In addition, some small satellite peaks appeared at about 130.0 ppm in AEOL, suggesting that some condensed lignin or derivatives, appeared after the AEOP process. Meanwhile, the structural features of residual lignin in crude pulp (P-EMAL) could be achieved by comparing the P-EMAL with the original EMAL. It was found that the P-EMAL was also heavily affected by AEOP process, as revealed by a decreased signal at 152.2 ppm and increased signal at about 148.0 ppm. However, the still remained signals for $\beta$-*O*-4 linkages implied that further delignification is needed. After AE process, it was found that the obtained P-AEL presented a similar spectral pattern as AEOL, suggesting that AE process removed more lignin fragments resulting from the AEOP process; however, a part of the residual lignin was not removed by this process. In contrast, most of the "residual lignin" in the crude pulp could be removed after AHP process, although a part of lignin could be collected as P-AHPL. The lower yield of the P-AHPL is attributed to the oxidative degradation during AHP process.

**Table 2. Quantification of the $^{13}$C-NMR Spectra of the Lignin Polymers**

| $\delta$ (ppm) | assignment | EMAL | AEOL | P-EMAL | P-AEL | P-AHPL |
|---|---|---|---|---|---|---|
| 155−142 | aromatic C−O | 2.12 | 1.97 | 1.99 | 1.94 | 2.06 |
| 142−124 | aromatic C−C | 1.54 | 1.94 | 1.75 | 1.90 | 1.89 |
| 124−102 | aromatic C−H | 2.39 | 2.10 | 2.26 | 2.14 | 2.06 |
| 61.3−58 | $\beta$-$O$-4 | 0.75 | 0.29 | 0.63 | 0.36 | 0.50 |
| 57−55 | $CH_3O$ | 1.70 | 1.36 | 1.68 | 1.44 | 1.56 |

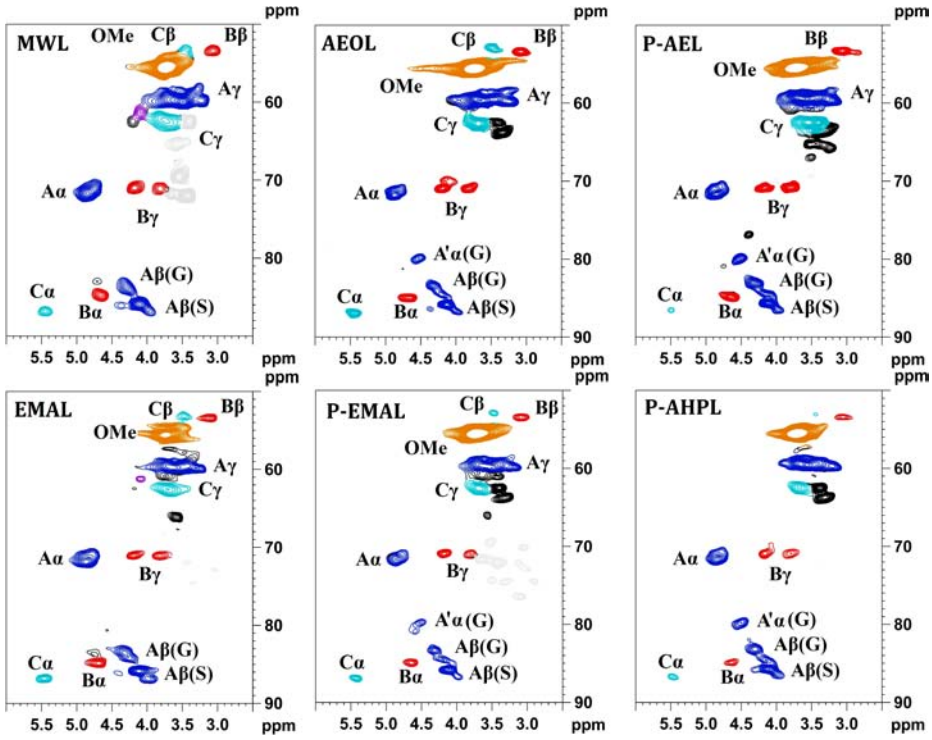


**Figure 3.** 2D-HSQC NMR spectra (Side-chain region) of lignin samples isolated from *Eucalyptus* wood after the integrated delignification processes. Lignin correlations are labeled with color-coded structures as given in Figure 5.

Quantification of the lignin fractions can give more precise structural evolution of lignin during integrated delignification process (Table 2). It was found that the amount of oxygenated carbons per aryl unit in AEOL (1.97/Ar) was decreased as compared to EMAL (2.12/Ar). In addition, the content of carbon−carbon (C−C) linkages in AEOL (1.94/Ar) was increased while the corresponding content of protonated aromatics was decreased (2.10), implying AEOL contained more C−C linkages, such as $\beta$−$\beta$ and $\beta$-5 linkages. Similarly, the integration values of corresponding regions in P-EMAL and P-AEL were similar to that of AEOL, implying that the crude pulp was affected greatly by AEOP process, which induced to form more C−C linkages. However, the P-AHPL contained intermediate value of C−C linkages between P-EMAL and EMAL, suggesting that the structural feature of P-AHPL was more similar to that of original EMAL. It also means that most of lignin resulting from the AEOP process undergone oxidative degradation in AHP process and could not be collected in this study. Another important issue should be noted was the content of $\beta$-$O$-4 linkages in these lignin polymers. The content of $\beta$-$O$-4 linkages in EMAL was 0.75/Ar, while it was decreased to 0.29/Ar in AEOL. For the P-EMAL, the value was 0.50/Ar, which was less than original EMAL but more than AEOL. After AE process, the content of $\beta$-$O$-4 linkages in P-AEL was only 0.36/Ar, which was near to that of AEOL, suggesting that P-AEL was mostly affected by AEOP process. However, after AHP process, the content of $\beta$-$O$-4 linkages was increased to 0.63/Ar, implying that P-AHPL was less affected by AEOP process. The $OCH_3$ content was accordant as the content of $\beta$-$O$-4 linkages. A higher $OCH_3$ content was accompanied by a higher content of $\beta$-$O$-4 linkages. For instance, EMAL contained a higher content of $\beta$-$O$-4 linkages and methoxy group ($OCH_3$). In contrast, AEOL contained a lower content of $\beta$-$O$-4 linkages and methoxy group ($OCH_3$). In light of the interesting results, the demethoxylation reaction of lignin probably occurred during the AEOP process, since the integration of aromatic region of lignin remains stable although the lignin undergone different pretreatments.

2D-HSQC NMR Spectra. Lignin contours in the HSQC spectra (Figures 3 and 4) were assigned by comparison based on the previous literatures.[8,29−31] The main signals assignments are listed in Supporting Information Table S2, and the main linkages detected from the lignin polymers are depicted in Figure 5. In *Eucalyptus* MWL and EMAL, the main linkages, such as $\beta$-$O$-4 aryl ethers (A), resinols (B), phenylcoumarans (C), could be assigned.[8,29] Comparison of 2D-HSQC NMR spectra of the produced lignin and corresponding control lignin samples can help to understanding the AEOP and extended delignification processes. For example, the structural changes of lignin during AEOP process could be observed by comparing the differences in the spectra of MWL, EMAL, and AEOL. The new correlation at 80.0/4.55 ppm appeared in the spectrum of

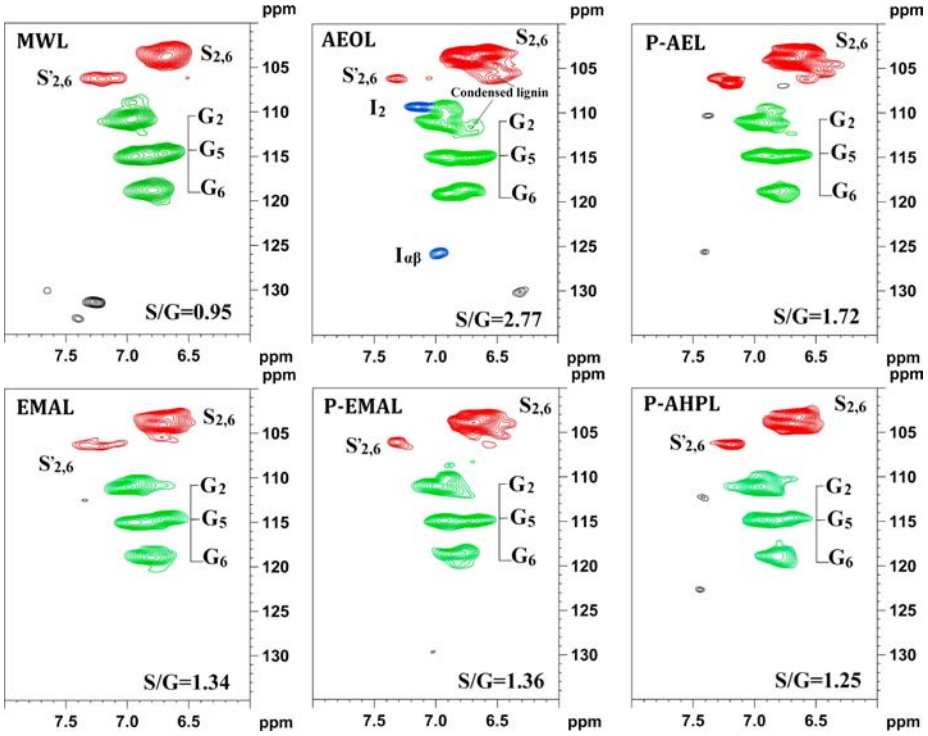


**Figure 4.** 2D-HSQC NMR spectra (Aromatic region) of lignin samples isolated from *Eucalyptus* wood after the integrated delignification processes.

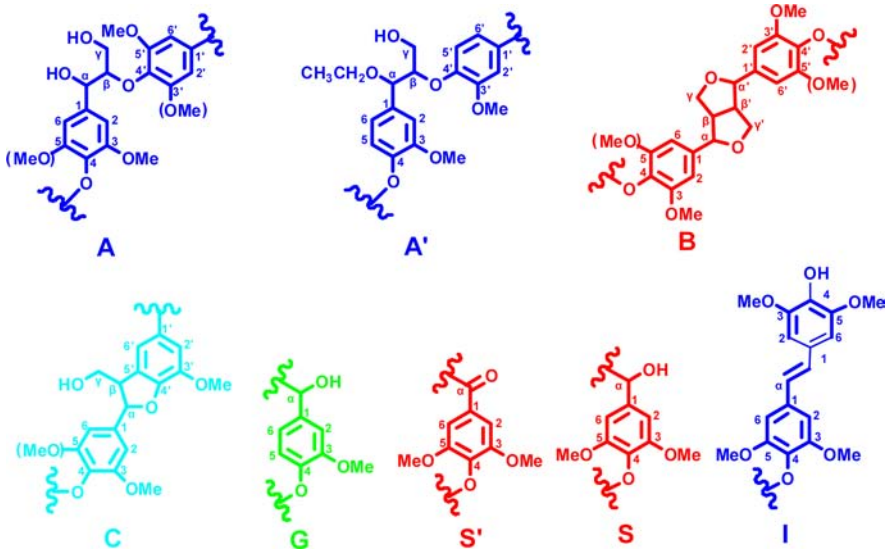


**Figure 5.** Main classical substructures, involving different side-chain linkages, and aromatic units identified by 2D NMR of *Eucalyptus* lignin obtained during the integrated process: (A) *β-O*-4 aryl ether linkages with a free −OH at the *γ*-carbon (blue) ; (A′) $C_\alpha$-ethoxylation *β-O*-4 linkages (blue); (B) resinol substructures formed by *β*−*β*, *α-O-γ*, and *γ-O-α* linkages (red); (C) phenylcoumarane substructures formed by *β*-5 and *α-O*-4 linkages (cyan); (I) stilbenes units (blue); (G) guaiacyl units (green); (S) syringyl units (red); (S′) oxidized syringyl units with a $C_\alpha$ ketone (red).

AEOL suggesting that *α*-ethoxylation occurred during AEOP process.[11] After extended delignification processes (AE and AHP), the *α*-ethoxylated *β-O*-4 (A′) still remained in the spectra of P-EMAL, P-AEL, and P-AHPL, implying that *α*-ethoxylation not only occurred in the released AEOL, but also appeared in the residual lignin in crude pulp (P-EMAL) and the subsequently removed lignin fractions (P-AEL and P-AHPL).

Aromatic regions of the HSQC spectra of these lignin samples can give basic composition of lignin. The correlated signals from syringyl (S/S′), and guaiacyl (G) lignin units were evidently presented. However, no *p*-hydroxyphenyl (H) units were detected in the spectra, which were in agreement with a previous report.[31] Two obvious signals at $\delta_C/\delta_H$ 109.0/7.15 and 126.0/7.00 ppm in AEOL were attributed to the $C_2$−$H_2$, $C_{\alpha/\beta}$−$H_{\alpha/\beta}$ of the stilbenes units. In addition, there were no obvious differences between these lignin samples.

Quantification of the lignin fractions by 2D-HSQC NMR method can provide explicit structural evolution during the integrated process. Herein, a quantification methodology was adopted in a recent review paper on lignin structures.[8] As shown in Table 3, the relative content of *β-O*-4 linkage in *Eucalyptus* MWL and EMAL was 72.2% and 70.3%,


dx.doi.org/10.1021/jf403717q | *J. Agric. Food Chem.* 2013, 61, 11067−11075

**Table 3. Quantification of the Lignin Polymers by Quantitative 2D-HSQC NMR**

| sample | β-O-4 | β−β | β-5 | S/G |
|---|---|---|---|---|
| MWL | 72.2 | 18.6 | 9.2 | 0.95 |
| EMAL | 70.3 | 20.6 | 9.1 | 1.34 |
| AEOL | 53.5 | 25.9 | 20.5 | 2.77 |
| P-EMAL | 64.1 | 20.3 | 15.6 | 1.36 |
| P-AEL | 64.7 | 30.3 | 5.0 | 1.72 |
| P-AHPL | 73.1 | 16.4 | 10.5 | 1.25 |

respectively. By contrast, the content of β-*O*-4 linkage reduced to 53.5% in AEOL, suggesting that β-*O*-4 linkage was cleaved greatly during the AEOP process. Meanwhile, the relative content of β-5 linkage was enhanced greatly, whereas β−β linkage was slightly increased as compared to MWL and EMAL, suggesting that more carbon−carbon linkages were formed, as also supported by the quantitative $^{13}$C NMR spectra of EMAL and AEOL aforementioned. The "residual lignin" in the crude pulp (P-EMAL) was also affected by AEOP process. The β-*O*-4 content in P-EMAL was decreased to 64.1% as compared to EMAL, while the contents of β−β and β-5 were similar to that of AEOL. After delignification with AE process, the P-AEL showed a similar content of β-*O*-4 content, but an increased content of β−β linkages and reduced β-5 content as compared to P-EMAL. The fact suggested that AE process probably selectively extracted the lignin fractions rich in β-*O*-4 and β−β linkages, which were composed of more S-type lignin units, as revealed by higher S/G ratios (syringyl to guaiacyl ratio).[32] By contrast, the relative content of β-*O*-4 linkage was enhanced after AHP process (P-AHPL), while the contents of β−β and β-5 were stable as compared to the MWL and EMAL of the raw material. The results suggested that the structural features of P-AHPL were similar to that of original EMAL. The S/G ratio of lignin in biomass is an important parameter in the delignification process. The S/G ratio of MWL was calculated to be 0.95 from 2D-HSQC spectra, whereas it was increased to 1.34 in EMAL. The reason for the increased S/G ratio could be explained by the following reasons: (1) Low yield of MWL may originate mainly from middle lamella, which contains fewer $OCH_3$ than in the secondary wall lignin ($S_2$).[33] (2) Higher yield of EMAL is probably originated mainly from middle lamella and second wall $S_2$ layer, the latter contains more syringyl units.[34] Thus, it is important to obtain representative lignin samples for understanding the original lignin in raw materials and pretreated substrates. By contrast, the S/G ratio in AEOL was 2.77, which was higher than those of MWL and EMAL. The higher S/G ratio of AEOL was attributed to the fact that AEOL was mainly composed of degraded lignin fragments, mainly including cleaved β-*O*-4 linkages, which was mainly formed by S-type lignin units in hardwood. In addition, a higher S/G ratio also implied that a condensation took place preferably at G units during AEOP. Besides, understanding S/G ratio of residual lignin in pulp will facilitate the subsequent delignification of the pulp. The S/G ratio of P-EMAL was 1.36, which was near to that of EMAL. Considering the similar S/G ratio and structural features of EMAL and P-EMAL, it was possible to deduce that extended alkaline delignification was needed since alkaline treatment selectively removes lignin with higher S/G ratios.[32] As expected, subsequent delignification with AE and AHP was demonstrated to be effective methods, especially AHP process. The higher S/G ratios of P-AEL (1.72) and P-AHPL (1.25) suggested that AE and AHP are all feasible in delignification process. However, AHP was more suitable based on the "similar compatible principle" because the S/G ratio and structural features of P-AHPL was similar to that of P-EMAL.

$^{31}$P NMR Spectra. To further investigate the structural changes of lignin during the integrated process, quantitative $^{31}$P NMR technique was also applied (Supporting Information Figure S7 and Table 4). For MWL and EMAL, the contents of S-type and G-type phenolic OH were lower and the content of S-type OH was less than that of G-type OH. This suggested that most of S-type lignin unit involves in the formation of β-*O*-4 linkages in these lignins and only a small amount of S−OH could be reacted with TMDP and detected by $^{31}$P NMR technique. After AEOP, the sharply enhanced S and G-type phenolic hydroxyl suggested that S and G-type phenolic OH was released after AEOP because of cleavage of β-*O*-4 linkages, as revealed by a lower content of β-*O*-4 linkages calculated from $^{13}$C NMR and 2D-HSQC spectra. The faster growth rate of S than G-type phenolic OH also implied that β-*O*-4 linkages were mainly composed of S units. In addition, the content of condensed S and G-type phenolic hydroxyls in AEOL was higher than that of EMAL and MWL, suggesting that AEOL has higher degree of condensation (DC), as mentioned in $^{13}$C NMR spectra. Moreover, the content of aliphatic OH was reduced greatly while the content of COOH was enhanced, suggesting that a part of aliphatic OH were oxidized into COOH during AEOP and other part of aliphatic OH was modified into α-ethoxylation, as mentioned in some publications.[11,35] Another, the reduced aliphatic OH and increased S-type phenolic OH in P-EMAL than EMAL also implied that P-EMAL was affected by the AEOP process, such as cleavage of β-*O*-4 linkages and α-ethoxylation. After AE process, the decreased aliphatic OH and the increased COOH probably implied that both the oxidation and α-ethoxylation occurred in the AE process. Similarly, the greatly increased

**Table 4. Quantification of the Lignin Polymers by Quantitative $^{31}$P-NMR Method**

| lignin | hydroxyl content (mmol/g of lignin) | | | | | | | |
|---|---|---|---|---|---|---|---|---|
| | aliphatic OH | syringyl OH | | guaiacyl OH | | *p*-hydroxy phenyl OH | carboxylic OH | total phenolic OH |
| | | C[a] | NC[b] | C | NC | | | |
| MWL | 4.83 | 0.24 | 0.11 | ND | 0.68 | 0.14 | 0.12 | 1.17 |
| EMAL | 5.46 | ND | 0.18 | 0.05 | 0.47 | 0.04 | 0.06 | 0.74 |
| AEOL | 2.32 | 0.26 | 1.25 | 0.20 | 0.90 | ND | 0.27 | 2.61 |
| P-EMAL | 3.67 | 0.13 | 0.66 | 0.16 | 0.50 | 0.01 | 0.05 | 1.46 |
| P-AEL | 2.40 | 0.12 | 0.67 | 0.19 | 0.49 | 0.02 | 0.54 | 1.49 |
| P-AHPL | 3.28 | 0.04 | 0.14 | 0.04 | 0.26 | 0.01 | 0.92 | 0.49 |

[a]C, Condensed. [b]NC, Noncondensed; ND, not detected.

content of COOH in P-AHPL was probably due to the oxidation of aliphatic OH and aromatic phenolic OH during AHP process. In addition, the content of S and G-type phenolic OH in P-AHPL was decreased as compared to P-EMAL, suggesting that S and G-type phenolic OH was also oxidized during the AHP process.

Molecular weights analysis. Figure 6 shows the curves of weight-average ($M_w$) and number-average ($M_n$) molecular

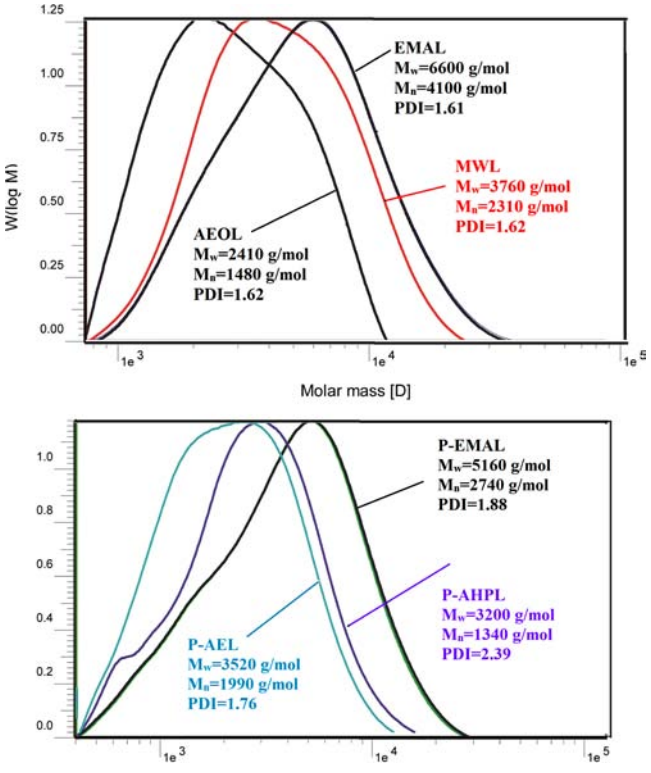


**Figure 6.** GPC curves of lignin polymers isolated from *Eucalyptus* wood chips.

weights as well as polydispersity index (PDI, $M_w/M_n$) of the lignin obtained after the integrated process. It was observed that EMAL has a bigger $M_w$ than that of MWL. The potential reasons are listed as below. Due to the limited solubility, only a small part of lignin fragments was extracted as MWL from the ball-milled powder, in contrast, large amounts of EMAL were extracted from the residue after enzymatic hydrolysis of the ball-milled wood, since the enzymatic hydrolysis removed most of carbohydrates, while lignin and small indigestible carbohydrates remained as residue. Thus, this facilitates the lignin extraction with 85% dioxane together with 0.01 M HCl at 85 °C. In addition, the addition of small amounts of HCl cleaved the bonds between the carbohydrates and lignin, thus the lignin with high molecular weights would be easily released. Thus, EMAL can be used as a representative "original lignin" from starting substrates. After AEOP, the $M_w$ was decreased to 2410 g/mol, which was significantly lower than that of EMAL. This suggested that the AEOP process degraded the "original lignin" in wood to a noticeable extent, which was also revealed by a reduced content of $\beta$-*O*-4 linkages as determined by quantitative $^{13}$C-, 2D-HSQC, and $^{31}$P NMR spectra. In addition, depolymerization and repolymerization of lignin are competitive reaction process under acidic conditions.[36] Although AEOL has a higher content of C−C bonds, it was deduced that depolymerization reaction was dominating the reaction during the production of AEOL when considering the lower $M_w$ of AEOL. Moreover, the $M_w$ of "original lignin" in crude pulp (P-EMAL) was 5160 g/mol. After AE and AHP processes, the $M_w$ were reduced to 3520 and 3200 g/mol, respectively. However, it was noted that P-AHPL presented a wide molecular weight distribution (PDI = 2.39), which was due to the oxidation of the AHP process.

In summary, *Eucalyptus* chips were successively treated with AEOP and subsequent delignification processes. After the integrated process, higher purity lignin polymers and cellulose (pulp) were successfully obtained. The integrated delignification with AEOP and AHP resulted in bleached pulp with lower lignin content (0.7%). The mechanism of the fundamental delignification of the *Eucalyptus* chips and crude pulp during the integrated process was illustrated by comparing the structural transformations of corresponding original lignin and released lignin polymers after these processes. It was observed that an extensive cleavage of $\beta$-*O*-4 linkages, $\alpha$-ethoxylation, transformation (stilbene unit), and some condensation reactions occurred in AEOL. Consequently, the subsequent delignification with AE was significantly affected by AEOP process. By contrast, AHP process can marvelously remove lignin from the crude pulp, obtaining the lignin (P-AHPL) similar to EMAL excepted for $\alpha$-oxidation. The well-defined structural features and chemical reactivity of the lignin polymers will maximize their ultimate utilizations in a future biorefinery scenario. Moreover, it is believed that investigating the fundamental chemistry of lignin during the integrated delignification process would be beneficial to optimize, control delignification process, and obtain high-purity lignin polymers and pulp.

## ■ ASSOCIATED CONTENT

### Supporting Information

Table S1. Yield and sugar content of the lignin obtained from the integrated delignification process. Table S2. Assignment of main lignin $^{13}$C−$^{1}$H cross-signals in the HSQC spectra of the lignin fractions. Figure S1. SEM pictures of pretreated *Eucalyptus* wood chips. Figure S2. XRD spectral patterns of pretreated *Eucalyptus* wood chips. Figure S3. CP-MAS $^{13}$C NMR spectra of pretreated *Eucalyptus* wood (amplifying spectra). Figure S4. CP-MAS $^{13}$C NMR spectra of AHP pretreated *Eucalyptus* wood and commercial MCC. Figure S5. FT-IR spectra of lignin isolated from *Eucalyptus* wood during the integrated process. Figure S6. Quantitative $^{13}$C NMR spectra of lignin samples isolated from *Eucalyptus* wood after the integrated delignification process (I). Figure S6. Quantitative $^{13}$C NMR spectra of lignin samples isolated from *Eucalyptus* wood after the integrated delignification process (II). Figure S7. Quantitative $^{31}$P NMR spectra of lignin samples isolated from *Eucalyptus* wood during the integrated delignification process. This material is available free of charge via the Internet at http://pubs.acs.org.

## ■ AUTHOR INFORMATION

### Corresponding Author

*Phone: +86-10-62336903. Fax: +86-10-62336903. E-mail: rcsun3@bjfu.edu.cn.

### Notes

The authors declare no competing financial interest.

## ■ ACKNOWLEDGMENTS

We are grateful for the financial support of this research from the National Natural Science Foundation of China (31110103902), Major State Basic Research Projects of China (973-2010CB732204), National 863 Project (863-2012AA023204), and Fundamental Research Funds for the Central Universities (BLYJ201313).

## ■ REFERENCES

(1) Pu, Y.; Zhang, D.; Singh, P. M.; Ragauskas, A. J. The new forestry biofuels sector. *Biofuels Bioprod. Biorefin.* **2008**, *2*, 58−73.

(2) Zhu, J.; Pan, X. Woody biomass pretreatment for cellulosic ethanol production: Technology and energy consumption evaluation. *Bioresour. Technol.* **2010**, *101*, 4992−5002.

(3) Chakar, F. S.; Ragauskas, A. J. Review of current and future softwood kraft lignin process chemistry. *Ind. Crops Prod.* **2004**, *20*, 131−141.

(4) Yuan, T. Q.; Xu, F.; Sun, R. C. Role of lignin in a biorefinery: Separation characterization and valorization. *J. Chem. Technol. Biotechnol.* **2013**, *88*, 346−352.

(5) Mansfield, S. D.; Kim, H.; Lu, F.; Ralph, J. Whole plant cell wall characterization using solution-state 2D NMR. *Nat. Protoc.* **2012**, *7*, 1579−1589.

(6) Ralph, J.; Landucci, L. L. NMR of lignins. In *Lignin Lignans*, Advances in Chemistry; Heitner, C., Dimmel, D., Schmidt, J., Eds.; CRC Press: Boca Raton, FL, 2010, pp 137−243.

(7) Pu, Y.; Cao, S.; Ragauskas, A. J. Application of quantitative $^{31}$P NMR in biomass lignin and biofuel precursors characterization. *Energy Environ. Sci.* **2011**, *4*, 3154−3166.

(8) Wen, J. L.; Sun, S. L.; Xue, B. L.; Sun, R. C. Recent advances in characterization of lignin polymer by solution-state nuclear magnetic resonance (NMR) methodology. *Materials* **2013**, *6*, 359−391.

(9) Zakzeski, J.; Bruijnincx, P. C.; Jongerius, A. L.; Weckhuysen, B. M. The catalytic valorization of lignin for the production of renewable chemicals. *Chem. Rev.* **2010**, *110*, 3552−3599.

(10) Quesada-Medina, J.; Lopez-Cremades, F. J.; Olivares-Carrillo, P. Organosolv extraction of lignin from hydrolyzed almond shells. *Bioresour. Technol.* **2010**, *101*, 8252−8260.

(11) Wen, J. L.; Xue, B. L.; Sun, S. L.; Sun, R. C. Quantitative structural characterization and thermal properties of birch lignins after auto-catalyzed organosolv pretreatment and enzymatic hydrolysis. *J. Chem. Technol. Biotechnol.* **2013**, *88*, 1663−1671.

(12) Oliet, M.; Rodríguez, F.; Santos, A.; Gilarranz, M. A.; García-Ochoa, F.; Tijero, J. Organosolv delignification of *Eucalyptus globulus*: Kinetic study of auto-catalyzed ethanol pulping. *Ind. Eng. Chem. Res.* **2000**, *39*, 34−39.

(13) Yáñez-S, M.; Rojas, J.; Castro, J.; Ragauskas, A. J.; Baeza, J.; Freer, J. Fuel ethanol production from *Eucalyptus globulus* wood by auto-catalized organosolv pretreatment ethanol-water and SSF. *J. Chem. Technol. Biotechnol.* **2013**, *88*, 39−48.

(14) Jaaskelainen, A. S.; Sun, Y.; Argyropoulos, D. S.; Tamminen, T.; Hortling, B. The effect of isolation method on the chemical structure of residual lignin. *Wood Sci. Technol.* **2003**, *37*, 91−102.

(15) Wu, S. B.; Argyropoulos, D. S. An improved method for isolating lignin in high yield and purity. *J. Pulp Pap. Sci.* **2003**, *29*, 235−240.

(16) Xiao, L. P.; Shi, Z. J.; Xu, F.; Sun, R. C. Characterization of lignins isolated with alkaline ethanol from the hydrothermal pretreated *Tamarix ramosissima*. *BioEnergy Res.* **2013**, *6*, 519−532.

(17) Sun, R. C.; Sun, X. F.; Wen, J. L. Fractional and structural characterization of lignins isolated by alkali and alkaline peroxide from barley straw. *J. Agric. Food Chem.* **2001**, *49*, 5322−5330.

(18) Yang, B.; Boussaid, A.; Mansfield, S. D.; Gregg, D. J.; Saddler, J. N. Fast and efficient alkaline peroxide treatment to enhance the enzymatic digestibility of steam-exploded softwood substrates. *Biotechnol. Bioeng.* **2002**, *77*, 678−684.

(19) Sun, R.; Sun, X.; Fowler, P.; Tomkinson, J. Structural and physico-chemical characterization of lignins solubilized during alkaline peroxide treatment of barley straw. *Eur. Polym. J.* **2002**, *38*, 1399−1407.

(20) Sluiter, A.; Hames, B.; Ruiz, R.; Scarlata, C.; Sluiter, J.; Templeton, D.; Crocker. D. *Determination of Structural Carbohydrates and Lignin in Biomass*, Technical Report, NREL/TP-510-42618, **2008**.

(21) Björkman, A. Studies on finely divided wood. Part I. Extraction of lignin with neutral solvents. *Sven. Papperstidn.* **1956**, *59*, 477−485.

(22) Wen, J. L; Sun, Y. C.; Meng, L. Y.; Yuan, T. Q.; Xu, F.; Sun, R. C. Homogeneous lauroylation of ball-milled bamboo in ionic liquid for bio-based composites production: Part I: Modification and characterization. *Ind. Crops Prod.* **2011**, *34*, 149−1501.

(23) Wen, J. L.; Sun, S. L.; Xue, B. L.; Sun, R. C. Quantitative structures and thermal properties of the birch lignins after ionic liquid-based biorefinery. *J. Agric. Food Chem.* **2013**, *61*, 635−45.

(24) Crestini, C.; Argyropoulos, D. S. Structural analysis of wheat straw lignin by quantitative $^{31}$P and 2D NMR spectroscopy. The occurrence of ester bonds and $\alpha$-O-4 substructures. *J. Agric. Food Chem.* **1997**, *45*, 1212−1219.

(25) Granata, A.; Argyropoulos, D. S. 2-Chloro-4, 4, 5, 5-tetramethyl-1, 3, 2-dioxaphospholane, a reagent for the accurate determination of the uncondensed and condensed phenolic moieties in lignins. *J. Agric. Food Chem.* **1995**, *43*, 1538−1544.

(26) Xu, Y.; Li, K.; Zhang, M. Lignin precipitation on the pulp fibers in the ethanol-based organosolv pulping. *Colloids Surf.* **2007**, *301*, 255−263.

(27) Mittal, A.; Katahira, R.; Himmel, M. E.; Johnson, D. K. Effects of alkaline or liquid-ammonia treatment on crystalline cellulose: Changes in crystalline structure and effects on enzymatic digestibility. *Biotechnol Biofuels* **2011**, *4*, 1−16.

(28) Faix, O. Classification of lignins from different botanical origins by FT-IR spectroscopy. *Holzforschung* **1991**, *45*, 21−28.

(29) Rencoret, J.; Gutiérrez, A.; Nieto, L.; Jiménez-Barbero, J.; Faulds, C. B.; Kim, H.; Ralph, J.; Martínez, Á. T.; José, C. Lignin composition and structure in young versus adult *Eucalyptus globulus* plants. *Plant Physiol.* **2011**, *155*, 667−682.

(30) Rencoret, J.; Marques, G.; Gutiérrez, A.; Nieto, L.; Santos, J. I.; Jiménez-Barbero, J.; Martínez, Á. T.; del Río, J. C. HSQC-NMR analysis of lignin in woody (*Eucalyptus globulus* and *Picea abies*) and non-woody (*Agave sisalana*) ball-milled plant materials at the gel state 10th EWLP, Stockholm, Sweden, August 25−28, 2008. *Holzforschung* **2009**, *63*, 691−698.

(31) Rencoret, J.; Marques, G.; Gutierrez, A.; Ibarra, D.; Li, J.; Gellerstedt, G.; Santos, J. I.; Jiménez-Barbero, J.; Martinez, A. T.; del Río, J. C. Structural characterization of milled wood lignins from different *eucalypt species*. *Holzforschung* **2008**, *62*, 514−526.

(32) Wen, J. L.; Sun, Z. J.; Sun, Y. C.; Sun, S. N.; Xu, F.; Sun, R. C. Structural characterization of alkali-extractable lignin fractions from bamboo. *J. Biobased Mater. Bio.* **2010**, *4*, 408−425.

(33) Hu, Z.; Yeh, T. F.; Chang, H.-m.; Matsumoto, Y.; Kadla, J. F. Elucidation of the structure of cellulolytic enzyme lignin. *Holzforschung* **2006**, *60*, 389−397.

(34) Whiting, P.; Goring, D. Chemical characterization of tissue fractions from the middle lamella and secondary wall of black spruce tracheids. *Wood Sci. Technol* **1982**, *16*, 261−267.

(35) Hu, G.; Cateto, C.; Pu, Y. Q.; Samuel, R.; Ragauskas, A. J. Characterization of switchgrass lignin after ethanol organosolv pretreatment. *Energy Fuels* **2012**, *26*, 740−745.

(36) Li, J.; Henriksson, G.; Gellerstedt, G. Lignin depolymerization-repolymerization and its critical role for delignification of aspen wood by steam explosion. *Bioresour. Technol.* **2007**, *98*, 3061−3068.